Mesolytic Scission of C−C Bonds in Radical Cations of Amino Derivatives: Steric and Solvent Effects

Przemyslaw Maslak,* William H. Chapman, Jr., Thomas M. Vallombroso, Jr., and Brian A. Watson

Contribution from the Department of Chemistry, The Pennsylvania State University, University Park, Pennsylvania 16802

Received August 9, 1995[⊗]

Abstract: The radical cations of 1,2-dialkyl-1-(4′-(dimethylamino)phenyl)-2-phenylethanes ($\mathbf{2}^{\bullet+}$) have been observed to undergo unimolecular cleavage of central C−C bonds. The observed enthalpies of activation are significantly lower than those measured for the homolysis of the corresponding neutral substrates. The entropies of activation are small or negative, despite production of fragments and partial freeing of rotational degrees of freedom upon fragmentation. These activation parameters are solvent dependent, generally decreasing in solvents with higher polarity in a self-conpensatory manner, leading to the free energies of activation (and rate constants) that remain constant in different solvents. The free energies of activation depend on strain present in the structures, with ca. 63% of the strain relatived in the transition state. The fragmentation reactions of $\mathbf{2}^{\bullet+}$ have activation energies that are on average 23 kcal/mol lower than those for homolysis of **2**. The observed activation of single bonds for scission has thermodynamics origins. The fragmentation reactions of radical cations are also compared to the fragmentation reactions of the analogous radical anions.

Addition or removal of electrons activates molecules for fragmentation, providing a useful method of breaking bonds that are quite strong in the neutral substrates.[1-3] For example, cleavage of C−C bonds in photochemically[4] or thermally[5] generated radical cations has recently attracted considerable attention. The radical cations formed in situ are usually present only in very low steady-state concentrations, and consequently the kinetic data are only rarely available.[6] Thus, quantitative mechanistic details of such reactions have been largely unexplored.

In most cases the initially generated radical cations have the unpaired electron in the π-system, and the fragmentation reaction is accompanied by removal of the electron density from the space between the scissile bond atoms, ultimately resulting in apportionment of electrons to the fragments:

$$^{\bullet+}\mathrm{A{-}B} \rightarrow \mathrm{A}^{+} + \mathrm{B}^{\bullet} \qquad (1a)$$

$$^{\bullet+}\mathrm{A{-}B} \rightarrow \mathrm{A}^{\bullet} + \mathrm{B}^{+} \qquad (1b)$$

The unimolecular fragmentation of radical ions (mesolytic cleavage)[7] may follow a homolytic (eq 1a) or heterolytic (eq 1b) mode, depending on the thermodynamic stability of fragments.[1,4b]

By analogy to the fragmentation reactions of radical anions described previously,[8] we have selected for study the homolytic mode of fragmentation (eq 1a), adjusting the strength of the scissile bond by increasing the steric strain around it. As shown before, even in this mode of cleavage there is a substantial charge transfer between the fragments in the transition state (TS) of the reaction.[9] Our strategy minimizes the influence of such TS polarization on the activation energy and allows us to directly compare the mesolytic fragmentations (both radical cations and anions) with the corresponding homolysis of neutral substrates.

The nitrophenyl compounds (**1**) of our previous study[8] can be converted to 4-(dimethylamino)phenyl derivatives, **2**, which yield directly observable radical cations[6ab] (Scheme 1). These radical cations undergo cleanly scission of the central C−C bond, providing an opportunity to extensively probe the kinetics,

⊗ Abstract published in *Advance ACS Abstracts*, December 1, 1995.

(1) Maslak, P. *Top. Curr. Chem.* **1993**, *168*, 1.

(2) Chanon, M.; Rajzmann, M.; Chanon, F. *Tetrahedron* **1990**, *46*, 6193.

(3) Savéant, J.-M. *Tetrahedron* **1994**, *50*, 10117.

(4) Leading references to fragmentation reactions of photogenerated radical cations: (a) Arnold, D. R.; Maroulis, A. J. *J. Am. Chem. Soc.* **1976**, *98*, 5931. (b) Popielarz, R.; Arnold, D. R. *J. Am. Chem. Soc.* **1990**, *112*, 3068. (c) Okamoto, A.; Snow, M. S.; Arnold, D. R. *Tetrahedron* **1986**, *42*, 6175. (d) Arnold, D. R.; Du, X.; Chen, J. *Can. J. Chem.* **1995**, *73*, 307. (e) Reichel, L. W.; Griffin, G. W.; Muller, A. J.; Das, P. K.; Ege, S. N. *Can. J. Chem.* **1984**, *62*, 424. (f) Davis, H. L.; Das, P. K.; Reichel, L. W.; Griffin, G. W. *J. Am. Chem. Soc.* **1984**, *106*, 6968. (g) Albini, A.; Mella, M. *Tetrahedron* **1986**, *42*, 6219. (h) Bardi, L.; Fasani, E.; Albini, A. *J. Chem. Soc., Perkin Trans. 1* **1994**, 545. (i) Ci, X.; Kellet, M. A.; Whitten, D. G. *J. Am. Chem. Soc.* **1991**, *113*, 3893. (j) Ci, X.; Whitten, D. G. In *Photoinduced Electron Transfer*: Fox, M. A., Chanon, M., Eds.; Elsevier: Amsterdam, 1988; Vol. C, p 553. (k) Schuster, G. B. In *Advances in Electron Transfer Chemistry*: Marino, P. S., Ed.; JAI Press Inc.: Greenwich, CT, 1991: Vol. 1, p 163. (l) Wang, Y.; Schanze, K. S. *J. Phys. Chem. Soc.* **1995**, *99*, 6876. (m) Akaba, R.; Niimura, Y.; Fukushima, T.; Kawai, Y.; Tajima, T.; Kuragami, T.; Negeishi, A.; Kamata, M.; Sakuragi, H.; Tokumaru, K. *J. Am. Chem. Soc.* **1992**, *114*, 4460.

(5) Leading references to fragmentation reactions in thermally generated radical cations: (a) Trahanovsky, W. S.; Brixius, D. W. *J. Am. Chem. Soc.* **1973**, *95*, 6778. (b) Baciocchi, E. *Acta Chem. Scand.* **1990**, *44*, 645. (c) Kim, E. K.; Kochi, J. K. *J. Org. Chem.* **1993**, *58*, 786. (d) Camaioni, D. M.; Franz, J. A. *J. Org. Chem.* **1984**, *49*, 1607. (e) Penn, J. H.; Deng, D. *J. Am. Chem. Soc.* **1991**, *113*, 1001. (f) Penn, J. H.; Deng, D.-L. *Tetrahedron* **1992**, *48*, 4823. (g) Schmittel, M.; Heinze, J.; Trenkle, H. *J. Org. Chem.* **1995**, *60*, 2726. (h) DiCosimo, R.; Szabo, H.-C. *J. Org. Chem.* **1988**, *53*, 1673. (i) Pardini, V. L.; Smith, C. Z.; Utley, J. H. P.; Vargas, R. R.; Viertler, H. *J. Org. Chem.* **1991**, *56*, 7305.

(6) (a) Maslak, P.; Asel, S. L. *J. Am. Chem. Soc.* **1988**, *110*, 8260. (b) Maslak, P.; Vallombroso, T. M.; Chapman, W. H., Jr.; Narvaez, J. N. *Angew. Chem., Int. Ed. Engl.* **1994**, *33*, 73. (c) Sankararaman, S.; Perrier, S.; Kochi, J. K. *J. Am. Chem. Soc.* **1989**, *111*, 6448. (d) Lucia, L. A.; Burton, R. D.; Schanze, K. S. *J. Phys. Chem.* **1993**, *97*, 9078. (e) Gan, H.; Leinhos, U.; Gould, I. R.; Whitten, D. G. *J. Phys. Chem.* **1995**, *99*, 3566. (f) Akaba, R.; Kamata, M.; Sakuragi, H.; Tokumaru, K. *Tetrahedron Lett.* **1992**, *52*, 8105.

(7) (a) Maslak, P.; Narvaez, J. N. *Angew. Chem., Int. Ed. Engl.* **1990**, *29*, 283. (b) Müller, P. *Pure Appl. Chem.* **1994**, 1077.

(8) Maslak, P.; Narvaez, J. J.; Vallombroso, T. M., Jr. *J. Am. Chem. Soc.* **1995**, *117*, 12373.

(9) Maslak, P.; Chapman, W. H., Jr. *J. Org. Chem.* **1990**, *55*, 6334. (b) Maslak, P.; Chapman, W. H., Jr. *Chem. Commun.* **1989**, *1809*. (c) Maslak, P.; Chapman, W. H. Jr. *Tetrahedron* **1990**, *46*, 2715.

0002-7863/95/1517-12380$09.00/0

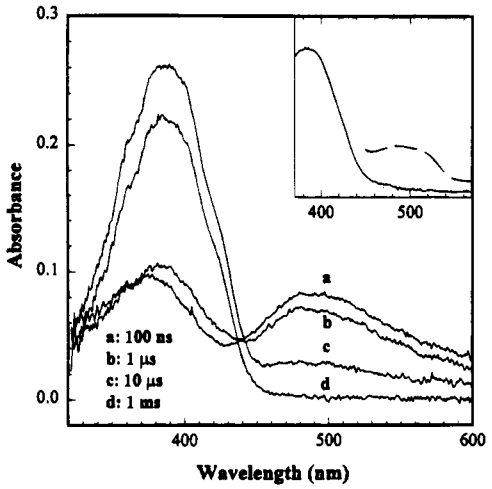

Figure 1. Transient absorbtion spectra of $\mathbf{2f}^{\bullet+}$ in CH_2Cl_2/5% MeOH recorded at 25 °C at different time intervals after the excitation (266 nm, 10 Hz, average of 100 pulses). Inset: Absorbance spectra of $\mathbf{2c}^{\bullet+}$ generated with TBPACA (−78 °C, CH_2Cl_2, broken line) and 4-(dimethylamino)cumyl cation obtained by optical electrochemistry (25 °C, 0.1 M TBAP in CH_2Cl_2, solid line).

Scheme 1

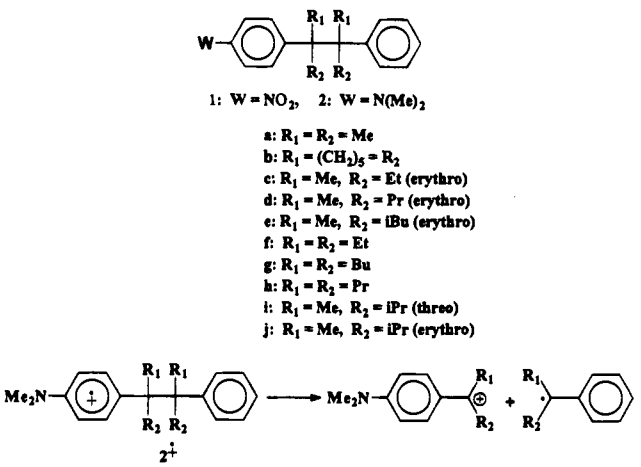

activation parameters, and effects of strain and solvent on the mesolytic processes. Here, we present results of such studies.

Results

The radical cations ($\mathbf{2}^{\bullet+}$) were generated by oxidation with tris(4-bromophenyl)aminium hexachloroantimonate[10] (TBPACA), electrochemical oxidation, or two-photon ionization in methylene chloride containing various polar additives, such as methanol, electrolyte salts, or other polar solvents. The method of generation depended on the half-life of the generated species. In the case of $\mathbf{2a,c,d,e}^{\bullet+}$ the radical cations were observed directly by ESR in CH_2Cl_2/5% MeOH. The ESR spectra were identical to that reported for (dimethylamino)-4-*tert*-butylbenzene radical cation[11] (a_N = 11.3 G, a_{NMe} = 12.2 G, a_{H_o} = 5.2 G, a_{H_m} = 1.3 G, a_{CMe} = 0.4 G). The radical cations of **2f,g,h** were observed by UV/visible spectroscopy in the flash-photolysis (FP) experiments (Figure 1). The radical cations had absorption maxima at 375 and 490 nm. Identical absorption bands were observed when 4-*tert*-butyl(dimethylamino)benzene was subjected to similar laser pulse (see below). The 490-nm maximum was confirmed by TBPACA oxidation of **1c** at −78 °C, whereat the radical cation ($\mathbf{1c}^{\bullet+}$) was persistent (the 375-nm region was obscured under these conditions; Figure 1, inset). All the neutrals showed oxidation waves in cyclic voltammetry (CV) at ca. 0.6−0.7 V vs SCE. The reversibility of the waves depended on experimental temperature (see Experimental Section) and scan rates.

All radical cations of **2** decayed in a first-order process. The observed rate constants were independent of the concentrations of the neutrals and the oxidized species. The decays corresponded to fragmentation of the central C−C bond as shown in Figure 1. The disappearance of radical cation absorbance was accompanied by the appearance of new strong absorbance at ca. 385 nm. This signal was assigned to the corresponding α,α-dialkyl-4-(dimethylamino)benzyl cation. The assignment was confirmed by independent generation of two cations of this series by electrochemical oxidation of 4,4′-bis(dimethylamino)-bicumene[12] (Figure 1, inset), giving the 4-(dimethylamino)cumyl cation (λ_{max} = 382 nm) or **2c** which yield 2-(4′-(dimethylamino)-phenyl)butyl cation (λ_{max} = 384 nm). The cations reacted with methanol present in the mixture as a cosolvent. No corresponding unsubstituted benzylic radicals or cations were detected in FP experiments. The CV traces obtained under conditions where the oxidation waves were irreversible, or only partially reversible, showed irreversible reduction peaks at ca. −0.35 V vs SCE (at 100 mV/s scan rates) corresponding to the reduction of the α,α-dialkyl-4-(dimethylamino)benzyl cations. The ESR spectra decayed to noise levels.

The results of product studies carried out in CH_2Cl_2/15% MeOH using TBPACA as oxidant were consistent with the cleavage leading to two benzylic fragments. In the case of $\mathbf{2a,e,f,g}^{\bullet+}$ the isolated fragments included α,α-dialkyl-4-(dimethylamino)benzyl methyl ethers, α,β-dialkyl-4-(dimethylamino)styrenes, α,α-dialkylbenzyl methyl ethers, and α,β-dialkylstyrenes. The styrenes were secondary products, derived from the corresponding methyl ethers by thermal elimination. No products with intact central C−C bonds were observed. The complete consumption of the starting amines required 2 equiv of oxidant (TBPACA). The details of these studies are provided in the Experimental Section.

The reversibility of the radical cation fragmentation was probed using **2c,e**. The starting materials recovered after partial cleavage of $\mathbf{2c,e}^{\bullet+}$ (1 equiv of oxidant added) showed no scrambling of stereochemistry (≤1% as compared to the authentic sample of the *threo* isomers)

The rates of cleavage and activation parameters were determined by ESR and FP in CH_2Cl_2/5% MeOH, as well as by CV in various solvents containing tetraethylammonium perchlorate (TEPA) or tetrabutylammonium perchlorate (TBAP) as electrolytes. The temperature range for each compound is reported in the Experimental Section. The data are collected in Table 1. In the kinetic ESR experiments, the radical cations were generated at low temperatures by electron transfer from **2** to TBPACA, and the signal intensity was followed over time. In FP experiments near room temperature, a solution of a donor (**2**) was pulsed with very high intensity UV light (266 nm, YAG laser), leading to a two-photon ionization of the material (the ejected electron is trapped by CH_2Cl_2). The monoexponential decays of the 490-nm band were used to obtain the kinetic data. In CV experiments carried out at temperatures where the oxidation waves were partially reversible the peak current ratio was used to obtain the kinetic data.[13]

To explore the effect of solvent on the rates and activation

(10) (a) Bell, F. A.; Ledwith, A.; Sherrington, D. C. *J. Chem. Soc.* C **1969**, 2719. (b) Schmidt, W.; Steckhan, E. *Chem. Ber.* **1980**, *113*, 577.

(11) Drews, M. J.; Wong, P. S.; Jones, P. R. *J. Am. Chem. Soc.* **1972**, *94*, 9122.

(12) Oxidative fragmentation of 4,4′-bis(dimethylamino)bicumene takes place via a dication mechanism.

(13) (a) Nicholson, R. S.; Shain, I. *Anal. Chem.* **1964**, *36*, 706. (b) Nicholson, R. S. *Anal. Chem.* **1966**, *38*, 1406.

Table 1. Kinetic Data for Homolysis and Mesolysis of **2a−j**

		homolysis[b]			mesolysis[c]			
	H_s[a]	$\Delta H^{\ddagger}_h$	$\Delta S^{\ddagger}_h$	$\Delta G^{\ddagger}_h$	k_m	$\Delta H^{\ddagger}_m$	$\Delta S^{\ddagger}_m$	$\Delta G^{\ddagger}_m$
2a	11.9	47.3	17	42.3	0.7	12.0	−18	17.5
		46.0	14	41.7		9.1	−23	16.0[d]
						[10.4]	[−23]	[17.2][d]
2b	13.2			(41.7)	[5.6]	[12.0]	[−15]	[16.5][d]
		47.6	18	42.2				
2c	15.1	48.5	27	40.5	20.0	15.6	1	15.3
		48.4	24	41.7		[14.0]	[−5]	[15.7][d]
						[6.5]	[−32]	[16.1][e]
2d	14.2			(38.8)	40.0	12.9	−7	15.0
		45.6	21	39.2		[7.3]	[−29]	[16.0][f]
2e	18.7	42.0	22	35.5	66.0	10.1	−12	13.7
		40.4	18	35.0		[5.5]	[−31]	[14.9][f]
2f	27.4	38.8	20	33.0	1.6×10^5	10.8	1	10.3
		41.9	26	34.0				
		44.7	34	34.5				
2g	22.3			(31.6)	5.4×10^5	8.9	−2	9.6
		38.2	22	31.6		[9.3]	[−4]	[10.6][g]
2h	24.6	37.8	21	31.4	4.4×10^5	8.2	−5	9.8
		34.9	13	31.0		[8.5]	[−9]	[11.1][g]
2i	29.4				*h*			
		35.1	14	30.8				
2j	29.7	*i*		(30.8)	[1.1×10^2]	[7.0	[−26]	[14.8][d]

[a] Strain energy in the hydrocarbon evaluated by molecular mechanics (ref 14) in kcal/mol. [b] Enthalpies (in kcal/mol) and entropies (in eu) of activation for homolysis of the hydrocarbons (in italics, ref 14) and the dimethylamino derivatives. The values in parentheses for the dimethylamino derivatives were extrapolated from the hydrocarbon data (see text). The estimated errors of determinations for the dimethylamino compounds are ±1 kcal/mol for enthalpies of activation and ±5 eu for activation entropies. The free-energy values are given at 300 K. [c] The rate constants (in s^{-1}) of mesolysis were measured in CH_2Cl_2/5% MeOH by ESR (**2a,c,d,e**$^{\bullet+}$) or flash-photolysis (**2f,g,h**$^{\bullet+}$), reported at 300 K. The enthalpies of activation (in kcal/mol) have an average error of ±0.9 kcal/mol and the entropies of activation (in eu) have errors of ±4 eu. The free energy of activation was calculated at 300 K. The data in brackets were obtained by CV in the presence of electrolyte. [d] 0.1 M TEAP in CH_3CN as solvent. [e] 0.1 M TBAP in CH_2Cl_2/MeOH (5%) as solvent. [f] 0.1 M TBAP in CH_2Cl_2 as solvent. [g] 0.2 M TBAP in butyronitrile/bromoethane (1:1) as solvent. [h] Not determined. [i] Compare to the nitro derivatives (ref 8).

parameters of mesolytic cleavage in more detail, the decay of **2a**$^{\bullet+}$ was measured by ESR in mixed solvents, containing CH_2Cl_2 and various amounts of a more polar component: MeOH, CF_3CH_2OH, *t*-BuOH, CH_3CN. Attempts to obtain kinetic data in pure solvents of different nucleophilicity and polarity were unsuccessful due to solubility problems or side reactions. Although the observed activation free energies were independent of the solvent used, the enthalpies and entropies of activation varied significantly with solvent composition. The data are collected in Table 2.

For comparison purposes the homolysis of neutrals, **2a,c,e,f,h**, was carried out in decaline or xylene containing a large excess of thiophenol serving as a radical scavenger. The consumption of the starting materials was followed by GC or HPLC. The observed fragments were identified as the corresponding α,α-dialkyltoluenes. The sample of **2e** recovered from partial cleavage (75% conversion) showed no scrambling of stereochemistry (≤1% of *threo* isomer was present), indicating irreversibility of homolysis. Kinetic data obtained at several temperatures covering the 40 °C range were used to obtain activation parameters for homolysis (Table 1). The activation energies calculated at 300 K were very similar to the data obtained for the corresponding hydrocarbons[14] (without aromatic substituents). The correlation between the amino derivatives and the hydrocarbons[14] ($\Delta G^{\ddagger}_h(NMe_2) = 0.96\Delta G^{\ddagger}_h(H) + 1.2$ (in kcal/mol), $r^2 = 0.97$) was employed to estimate data for the amino derivatives that were not studied in our laboratory.

Table 2. Activation Parameters[a] for Unimolecular Fragmentation of **2a**$^{\bullet+}$ in Methylene Chloride with Various Cosolvents

cosolvent[b] (% v/v)	$E_T(30)$[c] (kcal/mol)	$\Delta H^{\ddagger}_m$ (kcal/mol)	$\Delta S^{\ddagger}_m$ (eu)	$\Delta G^{\ddagger}_m$ (kcal/mol)[d]
none	41.6	18.1 ± 1.0	6 ± 4	16.6 ± 1.4
1% MeOH	43.9	16.3 ± 0.4	−4 ± 4	17.3 ± 1.1
3% MeOH	46.0	14.1 ± 1.0	11 ± 4	16.8 ± 1.4
5% MeOH	47.1	12.0 ± 0.4	−18 ± 2	16.4 ± 0.7
25% MeOH	51.1	11.7 ± 0.7	−22 ± 3	17.0 ± 1.0
50% MeOH	52.8	11.8 ± 0.7	−21 ± 4	16.9 ± 1.2
0.1% $CF_3CH_2CH_2OH$	47.0	16.7 ± 2.0	0 ± 7	16.8 ± 2.7
0.25% CF_3CH_2OH	48.8	14.3 ± 0.7	−11 ± 3	17.0 ± 1.0
0.5% CF_3CH_2OH	49.8	17.0 ± 2.0	1 ± 4	16.8 ± 2.2
1% CF_3CH_2OH	51.1	16.0 ± 1.0	−2 ± 5	16.5 ± 1.6
5% CF_3CH_2OH	54.0	15.9 ± 2.0	−4 ± 1	16.9 ± 2.0
10% CF_3CH_2OH	55.2	18.7 ± 1.0	8 ± 5	16.8 ± 1.6
1% *t*-BuOH	41.8	12.8 ± 1.0	−16 ± 5	16.6 ± 1.6
5% *t*-BuOH	42.1	14.3 ± 0.8	−9 ± 3	16.6 ± 1.1
8% *t*-BuOH	42.3	19.7 ± 1.0	13 ± 4	16.5 ± 1.4
15% *t*-BuOH	42.6	18.1 ± 0.2	5 ± 1	16.5 ± 0.3
1% CH_3CN	41.8	14.7 ± 0.5	−8 ± 4	16.7 ± 1.1
3% CH_3CN	41.9	14.7 ± 0.7	−8 ± 3	16.5 ± 1.0
6% CH_3CN	42.2	11.2 ± 0.4	−22 ± 2	16.6 ± 0.7
10% CH_3CN	42.5	13.8 ± 0.7	−11 ± 3	16.9 ± 1.0

[a] Determined by ESR in the −65 to −10 °C temperature range. [b] The values listed are v/v % of the added solvent. [c] Determined using Reichardt $E_T(30)$ dye (ref 23) in mixted solvents (Figure 3). The literature $E_T(30)$ values of pure solvents (ref 23) are as follows: CH_2Cl_2 40.7, MeOH 55.4, CF_3CH_2OH 59.8, *t*-BuOH 43.3, CH_3CN 45.6. [d] Calculated at the isokinetic temperature of 242 K.

Discussion

The neutral amino compounds readily underwent homolysis, reflecting the strain present in these structures.[14b] The homolytic reactions of dimethylamino derivatives (**2**) were very similar to those of nitro compounds[8] (**1**) and unsubstituted hydrocarbons studied by Rüchardt.[14] Not only were the activation energies for homolysis of the amino derivatives essentially equal to those of hydrocarbons, but also the respective enthalpies and entropies of activation were very close, showing less of the self-compensation phenomenon, which was observed[8] for **1**. The entropies of activation were characteristically large (17−27 eu) as expected for scission of a C−C bond[15] that is accompanied by freeing of rotational degrees of freedom around the alkyl side groups. We can safely conclude that aromatic substituents (dimethylamino or nitro) have an experimentally undetectable effect (in terms of $\Delta G^{\ddagger}_h$) on the homolysis of these substrates.[16]

The radical cations of **2** were easily produced by a variety of methods. The unpaired electron was localized on the (dimethylamino)phenyl moiety as evidenced by ESR and visible spectroscopy. The spectra were essentially identical to those observed for the radical cation of 4-*tert*-butyl-(dimethylamino)-benzene.[11] The electron jump from the unsubstituted ring was not kinetically significant as the activation energy of such a process[17] would be at least 34 kcal/mol, much more than any observed activation energy (see below). All radical cations studied (**2**$^{\bullet+}$) underwent rapid unimolecular cleavage of the

(14) (a) Kratt, G.; Beckhaus, H.-D.; Lindler, H. J.; Ruchardt, C. *Chem. Ber.* **1983**, *116*, 3235. (b) Kratt, G.; Beckhaus, H.-D.; Ruchardt, C. *Chem. Ber.* **1984**, *117*, 1748. (c) Kratt, G.; Beckhaus, H.-D.; Bernlöhr, W.; Ruchardt, C. *Thermochim. Acta* **1983**, *62*, 279. (d) Beckhaus, H.-D. *Chem. Ber.* **1983**, *116*, 86. (e) Beckhaus, H.-D.; Schoch, J.; Rüchardt, C. *Chem. Ber.* **1976**, *109*, 1369.

(15) Benson, S. W. *Thermochemical Kinetics*; J. Wiley: New York, 1976.

(16) A similar conclusion was reached by Rüchardt (ref 14b).

(17) The difference in the redox potentials between *tert*-butylbenzene (estimated at 2.2 V vs SCE, ref 17a,b) and 4-(dimethylamino)-*tert*-butylbenzene (0.71 V vs SCE) is 34 kcal/mol: (a) Howell, J. O.; Goncalves, J. M.; Amatore, C.; Klasinc, L.; Wightman, R. M.; Kochi, J. K. *J. Am. Chem.* **1984**, *106*, 3968. (b) Schlesener C. J.; Amatore, C.; Kochi, J. K. *J. Phys. Chem.* **1986**, *90*, 3747.

central C−C bond according to Scheme 1 as evidenced by kinetic and product studies. The flash-photolysis experiments (Figure 1) clearly indicated that the unimolecular fragmentation reactions yield the corresponding 4-(dimethylamino)-α,α-dialkylbenzyl cations and the α,α-dialkylbenzyl radicals (not directly observed). The kinetics of the radical cation decay (at 490 nm) was very similar to the kinetics of the cumyl cation growth (at ca. 383 nm). The cumyl cations formed in the cleavage reacted slowly (millisecond time scale) with MeOH present as cosolvent (Figure 1, trace d). The presence of an isosbestic point (at ca. 440 nm) attests to the "cleanness" of the transformation. The cumyl cations were also detected by CV in the form of irreversible reduction waves.

Under the conditions of flash-photolysis experiments (**2f,g,h**$^{\bullet+}$) the unsubstituted α,α-dialkylbenzyl radicals formed in the cleavage are not oxidized by the radical cation present (insufficient concentration and lifetime of **2**$^{\bullet+}$ to allow for bimolecular reactions). Under the conditions of the ESR and CV experiments the concentration of radical cations is higher and their lifetimes are longer (from seconds to minutes), allowing for at least partial oxidation of the α,α-dialkylbenzyl radicals by **2**$^{\bullet+}$ (or directly by the electrode). Under such circumstances the actual cleavage rate constants are 1−0.5 times the observed rates constants, depending on the degree of oxidation of the α,α-dialkylbenzyl radicals, which is close to full oxidation for the CV and ESR experiments as indicated by the product studies. This factor is not significant when the activation parameters are considered (it contributes at most 1.4 eu to the activation entropy). The rate constants presented in Table 1 are based on the observed values.

The products detected in the cleavage reactions indicate that both cumyl cations formed (one directly from cleavage, one by oxidation of the corresponding radical formed in the fragmentation process) are trapped by MeOH present in the medium, giving methyl ethers. In the absence of added nucleophiles the major products are the corresponding styrenes which also form in thermal reactions from the methyl ethers. In all attempts only products corresponding to the scission of the central C−C bond were observed. The cleavage reaction (**2c,e**$^{\bullet+}$) was found to be irreversible under the reaction conditions. The apparent irreversibility of this endergonic reaction (see below) indicates that there are other low activation-energy processes (such as radical coupling or oxidation) that successfully intercept the formed radicals and cations once they leave the solvent cage. Apparently, the cage escape efficiently competes with the stereochemistry scrambling that requires relative reorientation (rotation) of the fragments, or there is no cage recombination in these reactions.

The fragmentation reaction is mechanistically well defined and may serve as an excellent model of an elementary mesolytic process. The unpaired electron density that is initially localized on the aminophenyl ring must shift to the middle of the molecule as the reaction progresses. The near-perfect alignment[8,14b,18] of the σ-orbital of the scissile bond with the π-system bearing the unpaired electron facilitates the process[1] (for an apparent exception see below), ultimately resulting in the formation of the α,α-dialkyl-4-(dimethylamino)benzyl cations and α,α-dialkylbenzyl radicals (Scheme 1). The electronic similarity of all the ground state and transition structures throughout the series allows us to make a quantitative comparison of this mesolytic process with homolytic cleavages under conditions where the reaction is mostly controlled by steric and solvent (for the charged substrates) effects.

(18) (a) Maslak, P.; Narvaez, J. N.; Parvez, M. *J. Org. Chem.* **1991**, *56*, 602. (b) Littke, W.; Drück, U. *Angew. Chem., Int. Ed. Engl.* **1979**, *18*, 406.

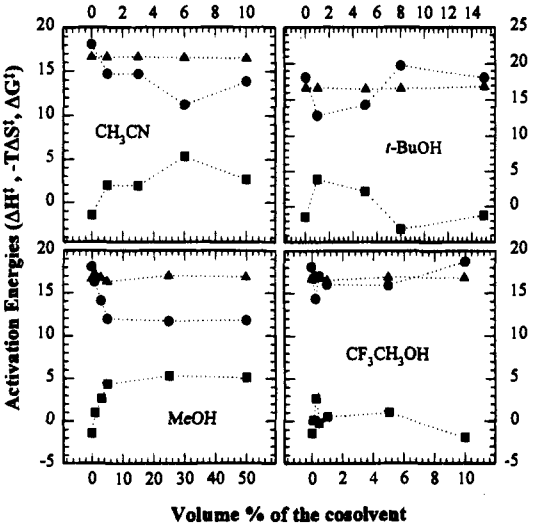

Figure 2. Solvent effect on activation parameters of fragmentation of **2a**$^{\bullet+}$ in CH_2Cl_2, containing various amounts of cosolvent (% v/v). The circles represent $\Delta H^{\ddagger}_m$, the squares $-T\Delta S^{\ddagger}_m$, and the triangles $\Delta G^{\ddagger}_m$ values calculated at the isokinetic temperature of 242 K. The data points are joined by dotted lines to clarify the trends.

The free energies of activation for fragmentation of **2**$^{\bullet+}$ are essentially solvent independent. In all cases studied, in solvents of different polarity and containing various polar additives the calculated values of $\Delta G^{\ddagger}_m$(300K) were identical within experimental error. This behavior points out that any comparison of cleavage reactions should be carried out in terms of free-energy quantities (where the solvent influences cancel) rather than in terms of enthalpies and entropies of activation which are strongly affected by the reaction environment. As a general observation, addition of polar additives (solvent, electrolyte) leads to lowering of $\Delta H^{\ddagger}_m$ and $\Delta S^{\ddagger}_m$ values in a self-compensating way. A similar trend was observed[8] for radical anions of **1**. The magnitude of the effect is dependent on the structure of the radical ions (substitution around the central carbons) and the polar additive.

The trend is not an artifact of the method used to obtain kinetic information as indicated by the data for **2a**$^{\bullet+}$ where both ESR and CV gave comparable results for reaction carried out in CH_3CN in the presence of TEAP, and as illustrated by the more extensive studies run in mixed solvents (see below). The observed changes (self-compensation)[19] are in most cases outside of the experimental errors, and can be quite dramatic. For example, in the case of **2c**$^{\bullet+}$ the addition of electrolyte to CH_2Cl_2/5% MeOH solution results in a 9-kcal/mol change in $\Delta H^{\ddagger}_m$ (or $T\Delta S^{\ddagger}_m$). Similar magnitudes of change in activation parameters are observed in mixed-solvent studies.

The cleavage of **2a**$^{\bullet+}$ carried out in CH_2Cl_2 with varying amounts of MeOH, CF_3CH_2OH, *t*-BuOH, and CH_3CN (Table 2, Figure 2) clearly illustrates the complexity of the self-compensation phenomena. The clearest trend is observed for MeOH. The activation enthalpy decreases rapidly from 18 kcal/mol in pure methylene chloride to 12 kcal/mol in the solvent mixture containing 5% (v/v) of MeOH. The entropy of activation becomes progressively more negative, the $-T\Delta S^{\ddagger}_m$ term fully compensating for the decrease in enthalpy of activation. Above 5% of MeOH the change in activation parameters stops. Effectively, around −30 °C the rate constants of the reaction remain unchanged in solvents containing varying amounts of methanol.

(19) (a) Grunwald, E.; Steel, C. *J. Am. Chem. Soc.* **1995**, *117*, 5687. (b) Leffler, J. E.; Grunwald, E. *Rates and Equilibria of Organic Reactions*; John Wiley and Sons: New York, 1963. (c) Linert, W.; Jameson, R. F. *Chem. Soc. Rev.* **1989**, *18*, 447. (d) Linert, W. *Chem. Soc. Rev.* **1994**, *23*, 429.

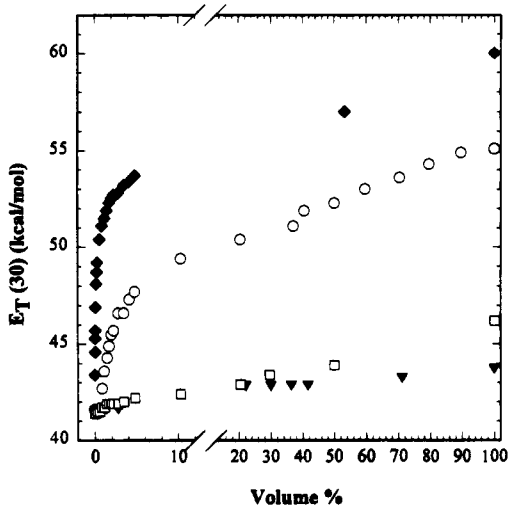

Figure 3. Experimentally determined changes in $E_T(30)$ values observed upon additions of selected solvents to CH_2Cl_2 displayed as a function of v/v % of the additive: CF_3CH_2OH filled diamonds, MeOH open circles, CH_3CN open squares, *t*-BuOH filled triangles.

This behavior is inconsistent with a nucleophilic substitution mechanism[20] observed for cyclopropyl derivatives[21a] or in cleavage of C−Si bonds,[21b] but some nucleophilic assistance in solvation of the incipient benzylic cation (specific solvation)[22] cannot be excluded. In this context, it is noteworthy that the most dramatic change in activation parameters takes place within the first 5% of added methanol. The $E_T(30)$ dye[23] studies of CH_2Cl_2/MeOH mixtures (Figure 3) show that nearly 50% of the total change in $E_T(30)$ values (from 0 to 100% of added MeOH) takes place within the first 5% of added alcohol, with only very gradual change at higher alcohol concentrations. Suggestively, the "magic" 5% v/v corresponds to ca. 1 molecule of MeOH (1.2 M) per 12 molecules of CH_2Cl_2 (14.8 M), i.e. close to one molecule of MeOH per solvent cage surrounding the dye molecule or the radical cation.[22]

When added to methylene chloride, the trifluoroethanol shows an even steeper raise in $E_T(30)$ values than methanol (Figure 3), but the changes in activation parameters in this case were not as dramatic, and showed a reversal of the trend at ca. 1%, followed by a relatively constant response at higher volumes of the additive. On the other hand, the enthalpies of activation decreased more slowly with increasing amount of acetonitrile added to the medium, and for *tert*-butyl alcohol the initial decrease in activation enthalpies was followed by a slow increase. In both these cases $E_T(30)$ changes relatively little over the range of concentrations studied (Figure 3). The observed trends in different solvents did not correlate with the $E_T(30)$ values of the solvent mixture.

Clearly the observed trends are quite complicated, and in addition to the specific solvation,[22] they may reflect "structure" building by the more polar component within the less polar solvent (CH_2Cl_2). It is not clear whether the solvent changes affect the ground state, the transition state, or both of these states. The ESR coupling patterns of $\mathbf{2a}^{\bullet+}$ in all solvents were essentially identical, with only minor changes in line widths, leading to a slightly better resolution of the smallest coupling constants in the case of CH_2Cl_2/CH_3CN. The constancy of the coupling patterns would suggest that the transition state is more affected than the ground state. However, since the nitrogen hyperfine couplings (and other coupling constants) in amine derived radical cations are not very sensitive to solvent changes[24] this conclusion must remain tentative. Both the ground state and the transition state are charged, but in the transition state the charge is more delocalized, i.e. shifted toward the benzylic carbons.[9] Effective specific solvation of these centers might be entropically costly due to steric shielding by the side alkyl groups. In agreement with this line of reasoning the most crowded members of the series have (on average) less negative entropies of activation, i.e. the solvent (polar additive) cannot penetrate close to the sites with high charge density.

Regardless of the underlying reason(s), the compensation[19] between enthalpies and entropies of activation is nearly perfect. In fact the isokinetic plot ($\Delta H^{\ddagger}_m$ vs $\Delta S^{\ddagger}_m$) for all the data of Figure 2 shows an excellent correlation ($r^2 = 0.99$) with the slope equal to the isokinetic temperature ($T = 242$ K), which is right in the middle of the experimental temperature range used for this study. The quality of this isokinetic relationship is directly observable in Figure 2, by "flat-line" correlations exhibited by $\Delta G^{\ddagger}_m$(242K) in all solvent mixtures.

With the dangers of overinterpretation now apparent, it is nevertheless instructive to point out some differences between activation parameters for homolysis and mesolysis of the amino compounds. In CH_2Cl_2/5% MeOH, the enthalpies of activation for mesolysis are 30−35 kcal/mol lower than the corresponding values for homolysis. That difference can be even larger in more polar environments. The bond activation (see below) obtainable by electron removal is, however, less because of unfavorable entropies of activation. By contrast to large positive values observed in homolytic reactions, the mesolytic cleavages exhibit very small or negative $\Delta S^{\ddagger}_m$ (2 to −18 eu) that can become very negative in solvents with polar additives, such as ammonium salt perchlorates. This trend of lower enthalpies of activation and smaller or negative entropies of activation for mesolytic reactions in $\mathbf{1}^{\bullet-}$ and $\mathbf{2}^{\bullet+}$ as compared to the corresponding homolytic data of the neutrals seems to be general. At its origin is the compromise between the activation of the bond due to electron addition or removal, and solvation of the ions produced.

The free energies of activation for homolysis (**1** and **2**) and mesolysis ($\mathbf{1}^{\bullet-}$ and $\mathbf{2}^{\bullet+}$) show a good correlation with the strain present[14b] in molecules. It can be argued that all the strain is accumulated in the middle of the molecule,[14] and the fragmentation reaction would release most of it in the transition state. This is indeed the case for homolytic scission of **2** (Figure 4) as indicated by the slope of the correlation line of 0.93. The activation energies for the dimethylamino compounds closely follow the trend observed for the nitro derivatives[8] (slope is 1.0 for **1**) as well as for the hydrocarbons.[14,25] In all cases the correlation does not hold for the most crowded members of the series. Although, the reasons for the odd behavior of **f** derivatives are unclear, the deviations for **i**,**j** are mostly due to the residual strain[14b] present in the fragments. Correcting for this strain (estimated at ca. 3 kcal/mol per radical)[14b] would place the data points for these derivatives directly on the

(20) For $\mathbf{2}^{\bullet+}$, the possibility of a biomolecular reaction with external nucleophiles has been minimized by the choice of quaternary benzylic carbons. The fragmentation reaction takes place in pure CH_2Cl_2 with similar rate, and the rate constants are independent of concentration of MeOH (or other added nucleophile).

(21) (a) Dinnocenzo, J. P.; Todd, W. P.; Simpson, T. R.; Gould, I. R. *J. Am. Chem. Soc.* **1990**, *112*, 2468. (b) Dinnocenzo, J. P.; Farid, S.; Goodman, J. L.; Gould, I. R.; Todd, W. P.; Mattes, S. L. *J. Am. Chem. Soc.* **1989**, *111*, 8973.

(22) The term specific solvation is meant to describe a specific interaction between a solvent molecule(s) and the radical cation, in distinction from a general (bulk) dielectric effect.

(23) Reichardt, C. *Solvents and Solvent Effects in Organic Chemistry*; VCH Publishers: Weinheim, 1988.

(24) Nelsen, S. F. In *Landolt-Börnstein, New Series*; Hellwege, K.-H., Ed.; Springer-Verlag: New York, 1980; Vol. 9, Part d2, p 22.

(25) Rüchardt offered a slightly different analysis for a larger set of the corresponding hydrocarbons (ref 14b).

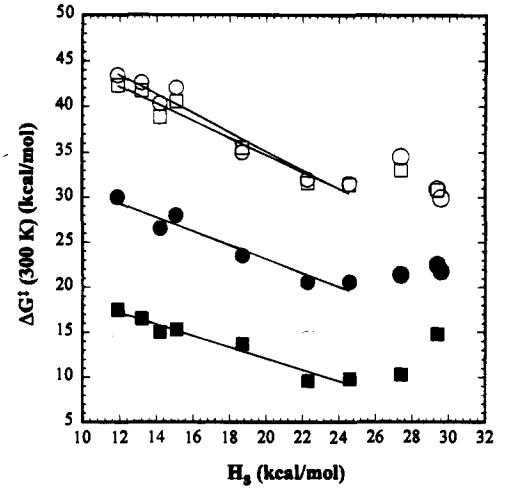

Figure 4. Plot of free energy of activation for homolysis (**1** open circles, **2** open squares) and mesolysis (**1**•− filled circles, **2**•+ filled squares) as a function of strain (H_s) present in the compounds. The most strained derivatives (**f**,**i**,**j**) have been excluded from the correlations. The correlations are the following. **1**: $\Delta G^{\ddagger}_h = -1.0H_s + 55.9$ ($r^2 = 0.95$). **2**: $\Delta G^{\ddagger}_h = -0.93H_s + 53.3$ ($r^2 = 0.96$). **1**•−: $\Delta G^{\ddagger}_m = -0.77H_s + 38.6$ ($r^2 = 0.94$). **2**•+: $\Delta G^{\ddagger}_m = -0.63H_s + 24.7$ ($r^2 = 0.95$). Data for **1** and **1**•− are from ref 8.

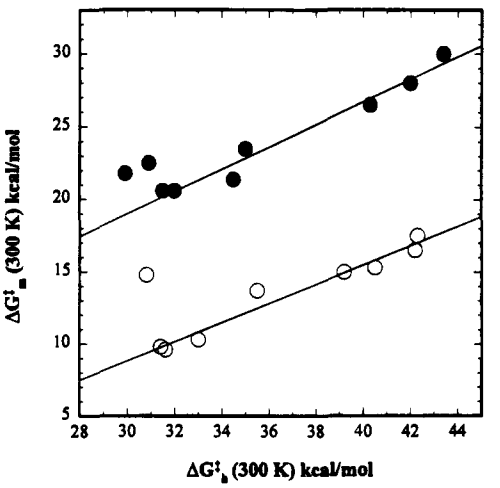

Figure 5. Correlation between the free energies of activation for homolysis and mesolysis. The data for **i**,**j** derivatives have been excluded from the least-squares lines. The filled circles represent data fom **1** and **1**•− (from the ref 8), and the open circles correspond to data for **2** and **2**•+. (**1**: $\Delta G^{\ddagger}_m = 0.77\Delta G^{\ddagger}_h - 4.2$ ($r^2 = 0.97$). **2**: $\Delta G^{\ddagger}_m = 0.67\Delta G^{\ddagger}_h - 11.2$ ($r^2 = 0.97$).)

correlation lines. Extrapolation of the correlation of **2** to strain-free compounds suggests that such a hypothetical derivative yielding two tertiary radicals upon homolysis would have $\Delta G^{\ddagger}_h$ of ca. 53 kcal/mol (56 kcal/mol for **1**), right in the middle of the estimate based on homolysis of bibenzyl (50−57 kcal/mol).[26,27]

The degree of strain release in the transition state for cleavage of **2**•+ is clearly less than that observed for homolysis of the neutrals. The slope of the correlation is only 0.63, even less than the slope of 0.77 observed for **1**•−. This observation is consistent with the Hammond postulate. The degree of bond breaking in the transition state that controls the amount of strain relieved is related to the endergonicity of the reaction (see below) that decreases from homolysis[14] (ΔG_h of 30−44 kcal/mol) to radical anion cleavage (ΔG_m of 15−26 kcal/mol)[6b] to radical cation fragmentation (ΔG_m of 6−14 kcal/mol).[6b] The solvent participation in the partitioning of activation parameters (see above) may also contribute to the diminished slope of the correlation. The strain is an enthalpic term, while the free energy of activation also contains entropic terms, which are affected by the identity of the side groups (and solvent).

The extrapolation of the correlation of Figure 4 to $H_s = 0$ gives $\Delta G^{\ddagger}_m$ for a hypothetical strain-free **2**•+ of ca. 25 kcal/mol, i.e., ca. 28 kcal/mol less than the corresponding homolytic activation free energy (see above). This difference in activation energies represents the maximum activation of the C−C bond available by electron removal in the dimethylamino systems. For comparison, the corresponding number for nitro derivatives is 17 kcal/mol (see below).

The free energy of mesolysis (**2**•+) correlates very well with the free energy of homolysis (**2**). The trend observed is similar to that found[8] for nitro derivatives (Figure 4). In both correlations **j** derivatives do not fit the correlation, although the deviation for **2j** is clearly much larger than that observed for **1j** (or its diasteroisomer, **1i**). As we have argued before,[8] the discrepancy indicates the presence of some extra contribution to the barrier in mesolytic reactions. The origin of this contribution is believed to be related to the rotational barrier[14a] that has to be (partially) overcome to bring the aromatic residues with unpaired electron into optimal overlap with the σ bond undergoing scission.[1,8,18] Apparently that contribution is more important for reactions with lower activation energies, i.e. with earlier, less-stretched transition states.

The average difference between the activation energies for homolysis and mesolysis of the amino derivatives is ca. 23 kcal/mol (excluding **2j**). The corresponding value for the nitro derivatives is ca. 12.5 kcal/mol, although the slope of the correlation (Figure 4) for the amino derivatives is only 0.67 as compared to 0.77 for the nitro compounds. As indicated above, at the limit of these correlations corresponding to strain-free compounds ($\Delta G^{\ddagger}_h \approx 55$ kcal/mol), the difference in activation energies for homolysis and mesolysis is 17 kcal/mol for the nitro compounds and 28 kcal/mol for the amino derivatives. The thermodynamic analysis[28] indicates that the maximum activation of the bond possible, ΔA, is ca. 16−17 kcal/mol for the radical anions and ca. 28 kcal/mol for the radical cations, disregarding the differences between the individual members of the series.[6b] Thus, we can conclude that at least in the case of unstrained derivatives, the transition states for mesolytic cleavages are lower in energy as compared to those for the homolytic reactions by the full difference in their thermodynamic driving forces. The lowering of activation energies in mesolytic reactions (as compared to homolysis) for actual members of the series is slightly less than the thermodynamically allowed maximum.[28] Nevertheless, it becomes apparent that the nearly parallel trends in activation energies observed for **1**•− and **2**•+ in Figures 4 and 5 have thermodynamic origins

(26) $\Delta H°_f$ of toluene is 11.9−12.4 kcal/mol (ref 27a,b), $\Delta H°_f$ of benzyl radical is 47−49 kcal/mol (ref 27c,d,e), $\Delta H°_f$ of cumene is 1.0 kcal/mol (ref 27a,b), $\Delta H°_f$ of cumyl radical is 32.4 kcal/mol (ref 27f). All values are at 298 K. Alternatively, C−H bond dissociation energy of toluene is given as 85−89 kcal/mol (ref 27d,e,g) and that of cumene as 83.5−84.4 kcal/mol (ref 27d,g). Both these reactions have very similar $\Delta S°$ values (ref 27g). $\Delta G^{\ddagger}_h$ (300 K) of bibenzyl is 60 kcal/mol (ref 27h).

(27) (a) Pedley, J. B.; Naylor, R. D.; Kirby, S. P. *Thermochemical Data of Organic Compounds*; Chapman and Hall: New York, 1986. (b) Benson, S. W.; Cruickshank, F. R.; Golden, D. M.; Haugen, G. R.; O'Neal, H. E.; Rodgers, A. S.; Shaw, R.; Walsh, R. *Chem. Rev.* **1969**, *69*, 279. (c) Lias, S. G.; Bartmess, J. E.; Liebman, J. F.; Holmes, J. L.; Levin, R. D.; Mallard, W. G. *J. Phys. Chem. Ref. Data* **1989**, *17* (Suppl.), 1. (d) McMillen, D. F.; Golden, D. M. *Annu. Rev. Phys. Chem.* **1982**, *33*, 493. (e) Rossi, M.; Golden, D. M. *J. Am. Chem. Soc.* **1979**, *101*, 1230. (f) Robaugh, D. A.; Stein, S. E. *Int. J. Chem. Kinet.* **1981**, *13*, 445. (g) Stein, S. E. *Structure and Properties*; National Institut of Standards and Technology, Standard Reference Data Program: Gaithersburg, 1994. (h) Stein, S. E.; Robaugh, D. A.; Alfieri, A. D.; Miller, R. E. *J. Am. Chem. Soc.* **1982**, *104*, 6567.

and the vertical shifts between their correlation lines correspond closely to the difference in driving forces for the two reactions.[6b,28] That shift ($\Delta G^{\ddagger}_{m}(\mathbf{1}^{\bullet-}) - \Delta G^{\ddagger}_{m}(\mathbf{2}^{\bullet+})$) averages ca. 11 kcal/mol (excluding the **j** derivative), an amount of energy almost exactly equal to the thermodynamically determined ΔA difference[28] ($\Delta A(\mathbf{2}^{\bullet+}) - \Delta A(\mathbf{1}^{\bullet-}) \approx 11-12$ kcal/mol, see above).

The parallel nature of the correlations observed for fragmentation of radical anions and cations indicates the similarity of bond activation mechanisms that can be realized by addition of electrons to the LUMO or by removal of electrons from the HOMO of neutral substrates. The presented data are an excellent starting point for a detailed analysis of the bond activation. Such analysis, in the form of free-energy relationships, will be presented elsewhere.[29]

Experimental Section

^{1}H NMR spectra were recorded on Bruker spectrometers, models WP-200 (200 MHz), AC-200 (200 MHz), AM-300 (300 MHz), or AM-360 (360 MHz). Chemical shifts are reported in ppm and referenced versus tetramethylsilane or the appropriate solvent peak. Ultraviolet/visible spectra were obtained on a Hewlett-Packard 8452 diode array spectrometer. Either a 1 cm quartz cuvette or a vacuum-jacketed variable-temperature cuvette was used. Mass spectra were recorded on a Kratos MS-950 double-focusing mass spectrometer (electron ionization, EI) or on a Kratos MS-25 double-focusing mass spectrometer using isobutane as the ionization gas (chemical ionization, CI). Only peaks of structural importance or those greater than 10% of the base peak are reported. Electron spin resonance spectra were obtained on a Varian E-Line spectrometer at 9 GHz using a Varian variable-temperature controller. The sample temperature was monitored using a copper–constantan thermocouple (Omega) inserted into the sample tube and connected to an Omega model 680 thermocouple thermometer.

Infrared spectra were recorded on either a Perkin-Elmer model 281 B infrared spectrometer or a Mattson 4020 Galaxy series Fourier transform infrared spectrometer. Spectra are reported in cm^{-1} and intensity is indicated as strong (s), medium (m), or weak (w). Electrochemical measurements were performed on a BAS-100A electrochemical analyzer connected to either a Bioanalytical Systems cell stand or to a variable-temperature cell. A three-electrode system was used, utilizing a saturated calomel (SCE), Ag/AgCl, or silver wire reference electrode, a platinum wire auxiliary electrode, and a Pt disc as the working electrode. The working electrode was polished on a felt pad with alumina prior to use. Ferrocene was employed as an internal standard to correct potentials to SCE. Unless otherwise stated, solutions were 0.1 M in tetraethylammonium perchlorate (TEAP) or 0.1 M tetrabutylammonium perchlorate (TBAP), and were sparged with argon prior to use.

Analytical gas chromatography was performed on a Varian model 3700 gas chromatograph equipped with 50- (column A) and 100-cm (column B) columns packed with 5% OV-101 on Supelcoport. In a typical run, the column was maintained at an initial temperature for several minutes, the temperature was then increased at a specific rate, and a final temperature was maintained for some time. GC retention times are reported along with a program designated as follows: initial temperature in °C, initial time in min, rate of increase in °C/min final temperature in °C, final time in min, and column. Results were recorded using a Hewlett-Packard model 3390-A integrator.

Analytical and preparative HPLC was performed on a Rainin Rabbit HPLC system fitted with a silica column, a Knauer variable-wavelength monitor (set at 254 nm), a Shimadzu C-R3A Chromatopac integrator, and a Rheodyne 7125 sample injector. Flash chromatography was performed using Merck silica gel 60. Analytical and preparative TLC was run on EM Science precoated silica gel plates with fluorescent indicator. Analytical TLC was performed on 0.25-mm plates and preparative work was done on 1.0-mm-thick plates.

All materials were obtained from Aldrich Chemical Co. unless otherwise stated, and were of the best quality available. Ether and THF were distilled from potassium metal under an argon atmosphere, using benzophenone as an indicator. Methylene chloride was distilled from calcium hydride under argon just prior to use. Acetonitrile used for electrochemical measurements was Aldrich anhydrous grade, and it was used without further purification. Tetrabutylammonium perchlorate was obtained from Kodak and was recrystallized twice from water and dried in a vacuum oven at 80 °C for 24 h. Tetraethylammonium perchlorate was obtained from the same source and was recrystallized from ethanol and dried under vacuum overnight. Solvents for UV–vis spectroscopy were spectrophotometric or HPLC grade from J. T. Baker.

Preparation of 2. Preparation of **2** involved reduction of the corresponding nitro compounds[8] (**1**) to amines which were methylated under reductive conditions with formaldehyde[30] without further purification. The general reduction procedure involved hydrogenation of **1** in ethyl acetate under 60 psi of H_2 in the presence of catalytic palladium on carbon (10%), or treatment of **1** in 95% ethanol with hydrazine in the presence of the same catalyst. Yields for both methods were comparable and ranged from 80 to 100%.

The aminobicumenes were converted to the desired dimethylamino compounds (**2**) by treatment with formaldehyde/sodium cyanoborohydride in acetonitrile.[30] Recrystallization from absolute ethanol afforded the pure products in good yields.

2-(4′-(Dimethylamino)phenyl)-3-phenyl-2,3-dimethylbutane (2a) was produced by hydrogenation of **1a** that gave 2-(4′-aminophenyl)-3-phenyl-2,3-dimethylbutane in 92% yield (mp 125–127 °C). **^{1}H NMR** ($CDCl_3$, 200 MHz): 7.16 (m, 3H), 7.1 (m, 2 H), 6.86 (d, J = 8 Hz, 2 H), 6.55 (d, J = 8 Hz, 2 H), 3.2 (s, br, 2 H), 1.3 (s, 6 H), 1.28 (s, 6 H). This amine after methylation gave a white solid (78% yield, mp 115–116 °C). **^{1}H NMR** ($CDCl_3$, 200 MHz): 7.06 (m, 5 H), 6.88 (d, J = 8 Hz, 2 H), 6.55 (d, J = 8 Hz, 2 H), 2.87 (s, 6 H), 1.24 (s, 6H), 1.22 (s, 6 H). **IR** (KBr): 2960 (m, 2775 (w), 1600 (m), 1510 (m), 1465 (w), 1435 (m), 1360 (s), 1330 (s), 1180 (m), 785 (s), 670 (m). **EI–MS** (*m/e*, relative intensity): 281 (M^+, 0.2%), 163 (12%), 162 (100%), 119 (3%).

1-(4″-(Dimethylamino)phenyl)-1′-phenyl-1,1′-bicyclohexane (2b) was produced by hydrogenation of **1b** that gave 1-(4″-aminophenyl)-1′-phenyl-1′-phenyl-1,1′-bicyclohexane in 93% yield (mp 135–139 °C). **^{1}H NMR** ($CDCl_3$, 300 MHz): 7.17 (m, 3 H), 6.99 (m, 2 H), 6.73 (d, J = 9 Hz, 2H), 6.56 (d, J = 9 Hz, 2 H), 3.51 (s, br, 2 H), 2.25 (m, 4 H), 1.40 (m, 10 H), 1.07 (m, 6 H). This amine after methylation gave a white solid (76% yield, mp 199–203 °C). **^{1}H NMR** ($CDCl_3$, 300 MHz): 7.17 (m, 3 H), 7.01 (m, 2 H), 6.83 (d, J = 9 Hz, 2 H), 6.61 (d, J = 9 Hz, 2 H), 2.94 (s, 6 H), 2.26 (m, 4 H), 1.39 (m, 10 H), 1.1 (m, 6 H). **CI–MS** (*m/e*, relative intensity): 362 ($(M + H)^+$, 8%), 202 (100%), 134 (13%), 91 (10%). **FTIR** (KBr): 2944 (s), 2926 (s), 2876 (s), 1615 (m), 1520 (s), 1474 (w), 1443 (w), 1348 (m), 1211 (w), 1165 (w), 806 (m), 704 (m).

***erythro*-3-(4′-(Dimethylamino)phenyl)-4-phenyl-3,4-dimethylhexane (2c)** was produced by reduction of **1c** with hydrazine that gave *erythro*-3-(4′-aminophenyl)-4-phenyl-3,4-dimethylhexane in 85% yield. **^{1}H NMR** ($CDCl_3$, 200 MHz): 7.15 (m, 3H), 6.97 (m, 2 H), 6.73 (d, J = 9 Hz, 2 H), 6.52 (d, J = 9 Hz, 2 H), 3.55 (s, br, 2 H), 2.17 (m, 2 H), 1.46 (m, 2 H), 1.27 (s, 3 H), 1.22 (s, 3 H), 0.58 (t, J = 7 Hz, 6 H). This amine after methylation gave a white solid (85% yield, mp 94–96 °C). **^{1}H NMR** ($CDCl_3$, 200 MHz): 7.17 (m, 3 H), 7.02 (m, 2 H), 6.84 (d, J = 9 Hz, 2 H), 6.59 (d, J = 9 Hz, 2 H), 2.90 (s, 6 H), 2.18 (m, 2 H), 1.43 (m, 2 H), 1.23 (s, 3 H), 0.58 (m, 6H). **FTIR** (KBr): 2971 (s), 2876 (m), 2799 (w), 1611 (m), 1522 (s), 1479 (m), 1343 (m), 1225 (w), 1169 (w), 1109 (w), 949 (w), 816 (m), 752 (w), 702 (s), 606 (w). EI-MS (*m/e*, relative intensity): 309 (M^+, 0.4%), 177 (13%), 176 (100%), 161 (8%), 134 (3%).

(28) Simple thermodynamic cycles (compare ref 6b) indicate that $\Delta G_m = \Delta G_h - 23.06\Delta E$ (in kcal/mol), where $\Delta E = E^{\circ}_{AB} - E^{\circ}_{A^{\bullet}}$(or $E^{\circ}_{B^{\bullet}}$) for radical cations, and $\Delta E = E^{\circ}_{A^{\bullet}}$(or $E^{\circ}_{B^{\bullet}}$) $- E^{\circ}_{AB}$ for radical anions, and all redox potentials (in V) refer to species in eq 1 of this or the previous paper (ref 8). For AB molecules where the electrons are removed from bonding orbitals or added to the antibonding orbitals, the radicals (A$^{\bullet}$ or B$^{\bullet}$) are easier to oxidize or reduce than AB species. Under such circumstances the ΔE term is always positive and is a measure of the maximum thermodynamically available redox activation (ΔA) for the scissile bonds in a given system as compared to the homolytic reaction (ΔG_h).

(29) The thermodynamics and free energy relationships for mesolysis will be discussed elsewhere: Maslak, P.; Vallombroso, T. M., Jr.; Chapman, W. H., Jr.; Narvaez, J. N. In preparation.

(30) Borch, R. F.; Hossid, A. I. *J. Org. Chem.* **1972**, *37*, 1673.

***erythro*-4-(4′-(Dimethylamino)phenyl)-5-phenyl-4,5-dimethyloctane (2d)** was produced by hydrogenation of **1d** that gave *erythro*-4-(4′-aminophenyl)-5-phenyl-4,5-dimethyloctane in 85% yield. **^{1}H NMR** ($CDCl_3$, 200 MHz): 7.16 (m, 3 H), 7.00 (m, 2 H), 6.76 (d, J = 9 Hz, 2 H), 6.53 (d, J = 9 Hz, 2 H), 3.53 (s, br, 2 H), 1.95 (m, 2 H), 1.50 (m, 2 H), 1.25 (s, 3 H), 1.20 (s, 3 H), 1.05 (m, 2 H), 0.80 (m, 8 H). This amine after methylation gave a white solid (67% yield, mp 65−68 °C). **^{1}H NMR** ($CDCl_3$, 200 MHz): 7.16 (m, 3 H), 7.00 (m, 2 H), 6.84 (d, J = 9 Hz, 2 H), 6.60 (d, J = 9 Hz, 2 H), 2.95 (s, 6 H), 1.97 (m, 2 H), 1.50 (m, 2 H), 1.25 (s, 3 H), 1.20 (s, 3 H), 1.05 (m, 4 H), 0.85 (m, 6 H). **CI−MS** (*m/e*, relative intensity): 338 ($(M + H)^+$, 12%), 190 (100%), 148 (8%). **FTIR** (KBr): 2951 (s), 2874 (m), 1613 (m), 1522 (s), 1443 (w), 1352 (m), 802 (m), 704 (s).

***erythro*-4-(4′-(Dimethylamino)phenyl)-5-phenyl-2,4,5,7-tetramethyloctane (2e)** was produced by hydrogenation of impure **1e** that gave *erythro*-4-(4′-aminophenyl)-5-phenyl-2,4,5,7-tetramethyloctane in 95% yield. **^{1}H NMR** ($CDCl_3$, 200 MHz): 7.15 (m, 2 H), 6.95 (m, 2 H), 6.7 (d, J = 9 Hz, 2 H), 6.5 (d, J = 9 Hz, 2 H), 3.56 (s, br, 2 H), 2.05 (m, 2 H), 1.13 (m, 4 H), 1.28 (s, 3 H), 1.23 (s, 3 H), 0.85 (m, 6 H), 0.65 (m, 6 H). This amine after methylation gave a white solid (33% yield, mp 124−127 °C). **^{1}H NMR** ($CDCl_3$, 200 MHz): 7.19 (m, 3 H), 6.97 (m, 2 H), 6.80 (d, J = 9 Hz, 2 H), 6.58 (d, J = 9 Hz, 2 H), 2.97 (s, 6 H), 2.06 (m, 2 H), 1.40 (m, 2 H), 1.20 (m, 2 H), 1.30 (s, 3 H), 1.25 (s, 3 H), 0.83 (m, 6 H), 0.64 (m, 6 H). **CI−MS** (*m/e*, relative intensity): 366 ($(M - H)^+$, 7.9%), 204 (100%), 161 (33%), 148 (12%), 121 (23%), 105 (27%). **FTIR** (KBr): 2957 (s), 2864 (m), 2795 (w), 1616 (m), 1524 (s), 1342 (m), 1169 (w), 949 (w), 816 (m), 702 (m).

3-(4′-(Dimethylamino)phenyl)-4-phenyl-3,4-diethylhexane (2f) was produced by hydrogenation of **1f** that gave 3-(4′-aminophenyl)-4-phenyl-3,4-diethylhexane in 100% yield. **^{1}H NMR** ($CDCl_3$, 200 MHz): 7.15 (m, 3 H), 7.00 (m, 2 H), 6.74 (d, J = 9 Hz, 2 H), 6.53 (d, J = 9 Hz, 2 H), 3.52 (s, br, 2 H), 1.94 (m, 8 H), 0.64 (m, 12 H). This amine after methylation gave a white solid (57% yield, mp 62−63 °C). **^{1}H NMR** ($CDCl_3$, 200 MHz): 7.15 (m, 3 H), 6.99 (d, J = 8 Hz, 2 H), 6.82 (d, J = 7 Hz, 2 H), 6.55 (d, J = 7 Hz, 2 H), 2.90 (s, 6 H), 1.95 (m, 8 H), 0.65 (m, 12 H). **CI−MS** (*m/e*, relative intensity): 338 ($(M + H)^+$, 6.3%), 190 ($(4\text{-}NMe_2C_6H_5C(C_2H_5)_2)^+$, 100%), 147 ($(C_6H_5C(C_2H_5)_2)^+$, 5.2%). **FTIR** (KBr): 3086 (w), 3052 (w), 2969 (s), 2936 (s), 2880 (s), 2807 (w), 1618 (s), 1524 (s), 1458 (m), 1358 (m), 1229 (w), 1169 (w), 1063 (w), 802 (s), 754 (m), 704 (s).

5-(4′-(Dimethylamino)phenyl)-6-phenyl-5,6-dibutyldecane (2g) was produced by reduction of **1g** with hydrazine that gave 5-(4′-aminophenyl)-6-phenyl-4,5-dibutyldecane in 76% yield. **^{1}H NMR** ($CDCl_3$, 200 MHz): 7.14 (m, 3 H), 6.98 (m, 2 H), 6.72 (d, J = 9 Hz, 2 H), 6.51 (d, J = 9 Hz, 2 H), 3.52 (s, br, 2 H), 1.86 (m, 8 H), 1.22 (m, 8 H), 0.97 (m, 4 H), 0.82 (m, 16 H). This amine after methylation gave a white solid (77% yield, mp 52−54 °C). **^{1}H NMR** ($CDCl_3$, 300 MHz): 7.12 (m, 3 H), 6.97 (m, 2 H), 6.79 (d, J = 9 Hz, 2 H), 6.55 (d, J = 9 Hz, 2 H), 2.91 (s, 6 H), 1.84 (m, 8 H), 1.21 (m, 8 H), 1.03 (m, 4 H), 0.86 (m, 4 H), 0.81 (m, 12 H). **CI−MS** (*m/e*, relative intensity): 450 ($(M + H)^+$, 5.1%), 246 (100%), 203 (37%), 190 (11%), 147 (10%), 134 (15%), 118 (10%), 91 (26%). **FTIR** (KBr): 2955 (s), 2928 (s), 2864 (m), 1613 (m), 1520 (s), 1464 (m), 1348 (m), 808 (m), 704 (m).

4-(4′-(Dimethylamino)phenyl)-5-phenyl-4,5-dipropyloctane (2h) was produced by reduction of **1h** with hydrazine that gave 4-(4′-aminophenyl)-5-phenyl-4,5-dipropyloctane in 93% yield. **^{1}H NMR** ($CDCl_3$, 200 MHz): 7.15 (m, 3 H), 7.00 (m, 2 H), 6.74 (d, J = 9 Hz, 2 H), 6.52 (d, J = 9 Hz, 2 H), 3.50 (s, br, 2 H), 1.80 (m, 8 H), 1.00 (m, 8 H), 0.80 (m, 12 H). This amine after methylation gave a white solid (72 yield, mp 94−96 °C). **^{1}H NMR** ($CDCl_3$, 200 MHz): 7.15 (m, 3 H), 7.00 (m, 2 H), 6.82 (d, J = 9 Hz, 2 H), 6.58 (d, J = 9 Hz, 2 H), 2.94 (s, 6 H), 1.84 (m, 8 H), 1.05 (m, 8 H), 0.82 (m, 12 H). **CI−MS** (*m/e*, relative intensity): 394 ($(M + H)^+$, 4%), 218 (100%), 175 (47%), 134 (11%), 91 (21%). **FTIR** (KBr): 3063 (w), 3088 (w), 2961 (s), 2868 (m), 2806 (w), 1613 (s), 1522 (s), 1470 (m), 1452 (m), 1362 (m), 1233 (w), 1167 (w), 953 (w), 810 (m), 758 (w), 698 (s).

ESR Experiments. ESR experiments were carried out in oven-dried glassware. Methylene chloride, acetonitrile, *tert*-butyl alcohol, and methanol were degassed by the freeze/pump/thaw method and stored over molecular sieves. Trifluoroethanol, bromoethane, and butyronitrile were used as received. Solutions were transferred using gas-tight syringes. A solution of the amino compound to be studied was prepared by weighing a small quantity of the material (2−5 mg) into a flask. The flask was fitted with a septum, evacuated, and flushed with argon. Enough solvent was then added to make a solution in a millimolar range (typically ca. 4 mM). A separate solution of the oxidant, TBPACA, of equivalent concentration was prepared in the same fashion.

ESR measurements were performed in a Pyrex tube (3 mm outer diameter) with a ground-glass joint capped with a Suba Seal septum through which a thermocouple wire had been inserted. The thermocouple (copper−constantan, 0.43 × 0.71 mm in a Teflon sleeve) was positioned with the tip 2 cm from the bottom of the tube. The tube was first evacuated, flushed with argon, and then washed with 0.1 mL of amine solution. It was then cooled to −78 °C (for **2a**,**c**) or −100 °C (for **2d**,**e**) and 0.050 mL of the amine solution was added. The oxidant solution (0.050 mL) was then added with mixing, and the tube was inserted into the precooled ESR cavity. At the beginning of each experiment, an ESR spectrum of the radical cation was obtained at a temperature at which there was no appreciable decay. The temperature was then increased, and the decay of the radical cation was followed by monitoring the decrease in signal intensity. Temperature fluctuation over the course of a run was less than 0.4 °C. The decays were fitted to zero-, first-, and second-order kinetic equations. All amino compounds studied displayed first-order kinetics. The solvent system used (CH_2Cl_2/5% MeOH) limits investigation to those compounds whose cleavage rates are measurable above −100 °C. Attempts to extend this range to lower temperatures using other solvent systems such as butyronitrile/bromomethane were unsuccessful. The specific temperature ranges were as follows: **2a**, −70 to −15 °C (−61 to −25 in 0.1 M TBPA/CH_2Cl_2); **2c**,**d**, −80 to −50 °C; **2e**, −103 to −80 °C.

The effect of solvent composition on the activation parameters for mesolysis was studied using $\mathbf{2a}^{\bullet+}$. Kinetic data for this compound were conveniently obtained by ESR techniques over a temperature range of −65 to −10 °C. The effect of solvent composition was studied in methylene chloride solution with varying percentages of methanol, acetonitrile, *tert*-butyl alcohol, and trifluoroethanol. Four to six different ratios of each mixture were used, the exact percentages depending on the identity of the minor component. At least six temperature points were used to construct the Eyring plot for each mixture.

Time-Resolved Optical Spectroscopy. Time-resolved optical spectroscopy (flash photolysis, FP) was used to obtained kinetic parameters for the most rapidly fragmenting radical cations ($\mathbf{2f,g,h}^{\bullet+}$). The experiments were performed using a Q-switched quantel Nd^{3+}-YAG laser to generate the transients. The laser, which produced a 10-ns-width pulse at a frequency of 10 Hz, was operated with flash lamps at full power. Transient spectra were generated by following a solution of the precursor (in 5% MeOH in CH_2Cl_2) through a 10 × 10 mm quartz cuvette at a flow rate of 1 mL/s. A 20-mL glass syringe was used to flow the solution. The cuvette, which was located in the path of the laser, was equipped with two fiber optic cables positioned 90° to the laser pulse. One cable was situated at the site of the pulse, and the other at an unexcited region. The transient was probed using a Xe flash lamp whose light was transferred via the fiber optic cables to the cuvette, and then on to a Spex Minimate monochromator set at the desired wavelength. A Princeton Instruments DIDA-512 dual diode array operated in gated mode was used to analyze the light from the monochromator when collecting transient spectra. During kinetic runs, the laser trigger signal was delayed using a multichannel digital delay. The delay setting controlled the time between the laser pulse and the flash from the Xe lamp used for detection. The time-dependent change in the absorbance was then monitored using a fast-responding two-channel photomultiplier tube connected to a digital oscilloscope. The temperature of the precursor solution was controlled by immersing the solvent reservoir into a bath of the desired temperature and then repeatedly flowing the solution through the system to allow it to equilibrate. The solution temperature was measured using a copper−constantan thermocouple inserted into the cuvette. A transient's spectrum or its decay was determined by averaging measurements from 50 to 100 laser pulses. The decay of the radical cations was monitored at 490 nm. The first-order rate constants derived from the temperature-dependent decays were used to construct Eyring plots from which the activation parameters were determined. The temperature range employed for **2f**,**g**,**h** was −10 to 32 °C.

Electrochemical Experiments. For electrochemical experiments, generally, 5 to 15 mg of analyte was weighed into an oven-dried vial along with enough solid electrolyte to make 10 mL of 0.1 M solution. The vial was then fitted to the cell stand and flushed with argon, and 10 mL of solvent was added. After placing the reference and working electrodes, the solution was sparged with argon for 3−5 min to remove oxygen and then maintained under a slight positive pressure for the remainder of the experiment. In some instances, small quantities of activated alumina were added to remove traces of impurities.

An optical electrode was prepared by sandwiching a fine gold mesh between two 1-mm-thick pieces of Teflon through which windows had been cut. The mesh was connected to a platinum wire lead with several layers of silver paint and the wire was held in place with a few drops of epoxy resin. The two pieces of Teflon were then wrapped with Teflon tape so that only the mesh in the window would be exposed to the electrolyte solutions. A silver wire insulated with Teflon tubing and held in place with Teflon tape a few millimeters from the mesh served as a pseudoreference electrode. A piece of Pt wire wrapped around the entire assembly acted as the auxiliary electrode. The electrode was connected via alligator clips to a power supply. In a typical experiment, the optical electrode was inserted into a vacuum-jacketed variable-temperature UV cell and the cell filled with 0.1 M electrolyte solution containing the precursor for the transient. A background spectrum was taken and stored and the potential was then ramped to a point beyond the redox potential of the precursor. Spectra were taken during the potential scan and stored. The final transient spectrum was obtained by subtraction of the precursor spectrum. A spectrum of the 4-(dimethylamino)cation was obtained by oxidative cleavage of 4,4-bis(dimethylamino)bicumene. Similarly, a solution of **2c** in 0.1 M TBAP/CH_2Cl_2 was electrolyzed between 0.8 and 1.0 V (SCE) to yield 2-(4′-(dimethylamino)phenyl)butyl cation (λ_{max} = 384 nm).

Kinetic parameters for mesolytic cleavage of **2** were obtained from partially reversible cyclic voltammetry data acquired in a variable-temperature electrochemistry cell. The temperature for study was one at which the analyte displayed at least partially reversible electrochemical behavior at scan rates below 20 V/s. Several cyclic voltammograms were subsequently run at various scan rates. Usually, four to eight voltammograms were collected at each temperature. In all cases the scan window was set so that the switching point was more than 100 mV beyond the redox potential of the compound. Data were collected at up to five different temperatures with a total range of 35−65 °C. The aminobicumenes were run in 0.1 M TEAP in acetonitrile (for temperatures down to −40 °C), 0.1 M TBAP in methylene chloride (down to −100 °C), or 0.2 M TBAP in 1:1 butyronitrile−bromoethane (for temperatures below −100 °C). Voltammograms were analyzed as described in the literature.[13] The specific conditions used were as follows. **2a**: 0 to 44 °C, 0.1 M TEAP/CH_3CN. **2b**: −28 to 26, °C 0.1 M TEAP/CH_3CN. **2c**: −10 to 25 °C, 0.1 M TEAP/CH_3CN; −85 to 0 °C, 0.1 TBAP/CH_2Cl_2-5% MeOH. **2d,e**: −53 to −80 °C, 0.1 TBAP/CH_2Cl_2. **2g,h**: −115 to −90 °C, 0.2 M TBAP/butyronitrile−bromoethane (1:1). **2j**: −42 to 25 °C, 0.1 M TEAP/CH_3CN.

Products. The products formed in the mesolytic cleavage of the amino compounds were investigated by reacting the compound of interest with TBPACA. Reactions run with 2 equiv of the oxidant resulted in ca. 50% conversion of starting amines. To quantitate the products better, 2 equiv of the oxidant were often used. The product identity and the *ratios* were the same after addition of 1 or 2 equiv of TBPACA. Typically, 20−50 mg of the amine was dissolved in enough methylene chloride/15% methanol to make a 20 mM solution, and the solution was cooled to −78 °C in a dry ice/acetone bath. One equivalent of the oxidant solution (in CH_2Cl_2) was added over several minutes. The mixture was stirred at −78 °C and then warmed to 0 °C. After being stirred for several minutes, the mixture was allowed to warm to room temperature. If desired the mixture was cooled back to −78 °C and the procedure was repeated with a second equivalent of oxidant solution. The resulting solution was washed with 1 M aqueous potassium hydroxide and dried over sodium sulfate. The components of the mixture were separated by HPLC or preparative TLC. The basic wash was necessary in order to recover products derived from the amino portion of the molecule. The procedure, however, led to production of styrene derivatives from the initially formed ethers. NMR studies on crude reaction mixtures (before basic wash) showed the presence of methyl ethers only (in addition to unreacted starting material and tris(4-bromophenyl)amine), indicating that the styrenes are not the products of the bond cleavage. The yields reported are based on isolated products corrected for the degree of conversion.

GC analysis of the reaction mixture obtained from **2a** prior to the hydroxide wash showed three peaks corresponding to α-methylstyrene (RT = 4.43, 50/03/15/280/05/B), 2-methoxy-2-phenylpropane (RT = 5.99), and tris(4-bromophenyl)amine (RT = 19.30). These assignments were made from the GC retention times of authentic samples. After the mixture was washed with aqueous potassium hydroxide, the components were separated by preparative TLC (1 mm thickness silica gel plate, 30% CH_2Cl_2 in hexane eluent). The products isolated were 2-methoxy-2-(4′-(dimethylamino)phenyl)propane (Rf = 0.21, GC RT = 9.51, 12%) and 2-methoxy-2-phenylpropane (Rf = 0.79, obtained as a mixture with tris(4-bromophenyl)amine). 2-Methoxy-2-(4′-(dimethylamino)phenyl)propane: **^{1}H NMR** ($CDCl_3$, 200 MHz) 7.30 (d, J = 9 Hz, 2 H), 6.72 (d, J = 9 Hz, 2 H), 3.03 (s, 3 H), 2.93 (s, 6 H), 1.5 (s, 6 H).

A proton NMR of the initial reaction mixture obtained from **2e** showed four major products in addition to the tris(4-bromophenyl)-amine. These were 2-(4′-(dimethylamino)phenyl)-4-methyl-2-pentene (46%), 2-(4′-(dimethylamino)phenyl)-4-methyl-1-pentene (46%), 2-methoxy-2-phenyl-4-methylpentane (49%), and 2-phenyl-4-methyl-1-pentene (25%). The mixture was then separated by HPLC (3% ethyl acetate/hexane). 2-(4′-(Dimethylamino)phenyl)-4-methyl-2-pentene (HPLC RT = 8.73, 36%): **^{1}H NMR** ($CDCl_3$, 200 MHz): 7.3 (d, J = 9 Hz, 2 H), 6.70 (d, J = 9 Hz, 2 H), 5.51 (d, J = 6 Hz, 1 H), 2.93 (s, 6 H), 2.67 (M, 1 H), 2.01 (s, 3 H), 1.03 (d, J = 7 Hz, 6 H). **CI−MS** (*m/e*, relative intensity): 203 (M^+, 100%), 188 (17%). 2-(4′-(Dimethylamino)-phenyl)-4-methyl-1-pentene (HPLC RT = 8.29, 33%): **^{1}H NMR** ($CDCl_3$, 200 MHz): 7.32 (d, J = 9 Hz, 2 H), 6.7 (d, J = 9 Hz, 2 H), 5.18 (s, 1 H), 4.86 (s, 1 H), 2.95 (s, 6 H), 2.34 (d, J = 7 Hz, 2 H), 1.7 (m, 1 H), 0.87 (d, J = 7 Hz, 6 H). **CI−MS** (*m/e*, relative intensity): 203 (M^+, 100%), 161 (19%), 85 (11%), 83 (16%). 2-Methoxy-2-phenyl-4-methylpentane (HPLC RT = 5.7, 21%): **^{1}H NMR** ($CDCl_3$, 200 MHz): 7.30 (m, 5 H), 3.08 (s, 3 H), 1.68 (m, 1 H), 1.57 (d, J = 6 Hz, 2 H), 1.56 (s, 3 H), 0.82 (d, J = 6 Hz, 3 H), 0.73 (d, J = 6 Hz, 3 H). **CI−MS** (*m/e*, relative intensity): 191 ($(M - H)^+$, 0.5%), 161 (54%), 135 (100%), 115 (16%).

The product mixture from reaction of **2f** was separated by preparative TLC (1 mm thickness silica gel plate, 30% CH_2Cl_2 in hexane eluent). The materials obtained were 3-methoxy-3-(4′-(dimethylamino)phenyl)-pentane (18%, Rf = 0.12, GC RT = 11.42, 50/03/15/280/05/B), 3-(4′-(dimethylamino)phenyl)-2-pentene (26%, Rf = 0.54, GC RT = 10.80), and tris(4-bromophenyl)amine. The presence of 3-methoxy-3-phenylpentane (GC RT = 8.10) could be inferred from a GC of the reaction mixture (as compared to an authentic sample) though the material was not isolated. 3-Methoxy-3-(4′-(dimethylamino)phenyl)pentane: **^{1}H NMR** ($CDCl_3$, 200 MHz): 7.27 (d, J = 9 Hz, 2 H), 2.44 (d, J = 9 Hz, 2 H), 3.02 (s, 3 H), 2.97 (s, 6 H), 1.83 (q, J = 7 Hz, 4 H), 0.73 (t, J = 7 Hz, 6 H). **CI−MS** (*m/e*, relative intensity): 221 (M^+, 54%), 189 (100%), 79 (17%), 69 (24%). 3-(4′-(Dimethylamino)phenyl)-2-pentene: **^{1}H NMR** ($CDCl_3$, 200 MHz): 7.25 (d, J = 9 Hz, 2 H), 6.70 (d, J = 9 Hz, 2 H), 5.64 (q, J = 7 Hz, 1 H), 2.94 (s, 6 H), 2.48 (q, J = 8 Hz, 2 H), 1.77 (d, J = 7 Hz, 3 H), 0.99 (t, J = 8 Hz, 3 H). **CI−MS** (*m/e*, relative intensity): 189 (M^+, 100%), 91 (10%), 79 (18%), 69 (27%), 62 (112%).

Four major products derived from **2g** were isolated by HPLC (3% THF in hexane). Isolated were 5-(4′-(dimethylamino)phenyl)-4-nonene (HPLC RT = 8.13, 78%), 5-methoxy-5-(4′-(dimethylamino)phenyl)-nonane (HPLC RT = 11.36, 7%), 5-phenyl-4-nonene (HPLC RT = 4.5, 24%), and 5-methoxy-5-phenylnonane (HPLC RT = 5.3, 43%, obtained as a mixture with tris(4-bromophenyl)amine). 5-(4′-(Dimethylamino)phenyl)-4-nonene: **^{1}H NMR** ($CDCl_3$, 300 MHz): 7.25 (d, J = 9 Hz, 2 H), 6.69 (d, J = 9 Hz, 2 H), 5.56 (t, J = 7 Hz, 1 H), 2.94 (s, 6 H), 2.45 (m, 2 H), 2.14 (m, 2 H), 1.45 (m, 2 H), 1.32 (m, 4 H), 0.92 (m, 6 H). **CI−MS** (*m/e*, relative intensity): 245 (M^+, 48%), 133 (12%), 83 (10%), 71 (100%). 5-Methoxy-5-(4′-(dimethylamino)phenyl)nonane: **^{1}H NMR** ($CDCl_3$, 300 MHz): 7.22 (d, J = 9 Hz, 2 H), 6.7 (d, J = 9 Hz, 2 H), 3.00 (s, 3 H), 2.904 (s, 6 H), 1.77 (m, 4 H), 1.27 (m, 4 H), 1.12 (m, 2 H), 0.95 (m, 2 H), 0.86 (t, J = 7 Hz,

6 H). **CI−MS** (*m/e*, relative intensity): 249 (M^+, 8%), 217 (55%), 206 (12%), 87 (10%), 71 (100%). 5-Phenyl-4-nonene: **^{1}H NMR** ($CDCl_3$, 300 MHz): 7.3 (m, 5 H), 5.64 (t, J = 7 Hz, 1 H), 2.15 (m, 4 H), 1.3 (m, 6 H), 0.87 (m, 6 H). **CI−MS** (*m/e*, relative intensity): 203 ($(M + H)^+$, 100%), 147 (24%), 145 (19%), 133 (14%), 118 (17%), 105 (10%), 91 (24%), 71 (34%), 69 (10%). 5-Methoxy-5-phenylnonane: **^{1}H NMR** ($CDCl_3$, 300 MHz): 7.25 (m, 5 H), 3.06 (s, 3 H), 1.81 (m, 4 H), 1.25 (m, 4 H), 1.09 (m, 4 H), 0.85 (t, J = 7 Hz, 6 H).

Homolytic Activation Parameters. Homolytic activation parameters for dimethylamino-substituted bicumyls were determined from an examination of the time-dependent disappearance of the materials in *cis*-decalin or xylene solutions with added thiophenol. Generally, a solution of the compound of interest (0.008−0.009 M in xylenes, *cis*-decalin, or a mixture of the two solvents) containing thiophenol (up to 20 equiv) was degassed by sparing with argon for 3−5 min. If the experiment was to be followed by GC, hexadecane was added in 1-μL increments (as an internal standard) until the intensity of the standard peak was comparable to that of the bicumene. The solution was then transferred to capillary tubes (40 μL per tube) and sealed under argon. The solutions were pyrolyzed by immersion in a temperature-regulated oil bath or a closely watched salt bath. Temperatures were regulated to within ±1.0 °C or better. At appropriate intervals samples were removed and rapidly cooled in a dry ice/acetone bath. Three to five samples per temperature were used to determine rate constants. Analysis of analyte concentration was performed by either GC or HPLC. In experiments followed by GC, the initial concentration of the bicumene was determined by injecting three 1-μL samples of the starting solution. The concentration was taken as being proportional to the ratio of the analyte to the internal standard. The concentration of each subsequent sample was determined by averaging the results from at least three injections. After the samples for each temperature run were complete, a sample of the original starting solution was again injected for comparison. In experiments analyzed by HPLC, a 10-μL sample from each tube was diluted in 5 mL of the elution solvent. A 20-μL sample of this solution was then injected on the HPLC. Determinations of concentration were an average of at least two injections. Again, at the completion of each temperature run a sample of the starting solution was injected for comparison. The rates obtained at at least four temperatures were used to construct the Eyring plots. The extent of reversibility for the thermolysis was examined by the partial thermolysis of **2e**. In this case the ampule was heated at 160 °C in an oil bath for 32.5 min, at which time HPLC (0.415% THF in hexane, retention time 7.06 min) showed only 25% of the starting amine remaining. The mixture was then diluted with 50 mL of diethyl ether, washed with 50 mL of 1 M aqueous potassium hydroxide, and dried over sodium sulfate. After concentration the components were separated by preparative TLC (eluted with 30% CH_2Cl_2 in hexane). The recovered starting material (R_f = 0.26) showed no *threo* isomer (less than 1% by NMR, as compared with an authentic sample).

Acknowledgment. This research was supported by a grant from NSF. The flash photolysis studies were carried out at the Regional Laser and Biotechnology Laboratories at the University of Pennsylvania supported by NIH. We thank Mark Phillips for his assistance in obtaining the time-resolved spectroscopy data.

JA952699S